Ultra-wideband linear-to-circular polarization conversion metasurface[*]

Bao-Qin Lin(林宝勤)[†], Lin-Tao Lv(吕林涛), Jian-Xin Guo(郭建新),

Zu-Liang Wang(王祖良), Shi-Qi Huang(黄世奇), and Yan-Wen Wang(王衍文)

School of Information Engineering, Xijing University, Xi'an 710123, China

An ultra-wideband and high-efficiency reflective linear-to-circular polarization conversion metasurface is proposed. The proposed metasurface is composed of a square array of a corner-truncated square patch printed on grounded dielectric substrate and covered with a dielectric layer, which is an orthotropic anisotropic structure with a pair of mutually perpendicular symmetric axes *u* and *v* along the directions with the tilt angles of $\pm 45°$ with respect to the vertical *y* axis. When the *u*- and *v*-polarized waves are incident on the proposed metasurface, the phase difference between the two reflection coefficients is close to $-90°$ in an ultra-wide frequency band, so it can realize high-efficiency and ultra-wideband LTC polarization conversion under both *x*- and *y*-polarized incidences in this band. The proposed polarization conversion metasurface is simulated and measured. Both the simulated and measured results show that the axial ratio (AR) of the reflected wave is kept below 3 dB in the ultra-wide frequency band of 5.87 GHz–21.13 GHz, which is corresponding to a relative bandwidth of 113%; moreover, the polarization conversion rate (PCR) can be kept larger than 99% in a frequency range of 8.08 GHz–20.92 GHz.

1. Introduction

Polarization is one of important characteristics of electromagnetic (EM) wave, and it must be taken into consideration in most practical applications. In various wireless systems, such as mobile communication, radar tracking, satellite communication and navigation systems, circularly polarized (CP) wave has been widely used due to the advantages such as simplifying alignment, overcoming Faraday rotation effect and multi-path fading.[1] To generate a desired CP wave, in addition to the way to generate it directly using CP antenna, an alternative effective way is to first generate a linearly polarized (LP) wave and then convert the LP wave into a CP wave by using a linear-to-circular (LTC) polarization converter.

Polarization converter is a kind of polarization control device, which can convert an incident wave with a given polarization into a reflected or transmitted wave with a different polarization. Polarization converter can be realized in different ways. Over the past decade, it has been found that metasurfaces can provide a convenient polarization control method for EM wave, which has aroused great concern. In recent years, many different polarization converters based on various metasurfaces have been proposed, which can perform different types of polarization conversions, such as reflective cross polarization conversion under LP[2–13] or CP[14–18] incidence, transmissive cross polarization conversion under

LP[19,21–23] or CP[24–26] incidence, and reflective[27–34] and transmissive[35–44] LTC polarization conversion under LP incidence. These metasurface-based polarization converters usually can be miniaturized, however, to date the existing literature has indicated that although a number of ultra-wideband reflective cross polarization converters have been proposed successfully, there are still few ultra-wideband LTC polarization converters proposed, moreover, previously proposed LTC polarization converters are still difficult to achieve these anticipated characteristics of ultra-wide band, high efficiency and compact structure at the same time. For example, Li *et al.* reported a transmissive LTC polarization converter using a bi-layered metasurface.[35] In addition, Gao *et al.* proposed a reflective LTC polarization converter using a micro-split Jerusalem-cross metasurface,[27] the operating frequency bands of the two polarization converter are 11.0 GHz–18.3 GHz and 12.4 GHz–21.0 GHz respectively, but their relative bandwidths are both only 50%. Later, a transmissive LTC polarization converter based on self-complementary zigzag metasurface was proposed by Baena *et al.*, in which the 3-dB axial-ratio (AR) relative bandwidth theoretically reaches 70.5%, however, in experiment, the bandwidth is still only 53%.[36] Meanwhile, Jiang *et al.* reported a reflective LTC polarization converter using a double-split square-ring metasurface in the terahertz regime, which can operate in a fre-

quency range of 0.60 THz–1.41 THz, the relative bandwidth is 80%.[28] Recently, a reflective LTC polarization converter using an ellipse-shaped metasurface was reported by Ran *et al.*, in which the AR of the reflective wave is lower than 3.0 dB in a frequency band of 10.21 GHz–24.97 GHz, and the relative bandwidth is only 83.91%.[29] Moreover, Fartookzadeh reported a reflective LTC polarization converter in terahertz regime, in which the 3-dB-AR-bandwidth reaches up to 116%, however, it is based on a three-layer rectangular-patch metasurface, and the polarization conversion rate (PCR) is still not very high.[30] As mentioned earlier, this kind of LTC polarization converter with the characteristics of ultra-wide band, high efficiency and compact structure still needs further studying.

In this work, a reflective metasurface is proposed, which can realize ultra-wideband LTC polarization conversion under both *x*- and *y*-polarized incidences. Its 3-dB axial ratio (AR) bandwidth reaches up to 113%, moreover, the PCR is kept larger than 99% in most part of the 3-dB-AR-band. The high-efficiency and ultra-wideband LTC polarization conversion performance of the proposed polarization converter is verified by both simulation and experiment; moreover, the root cause of the LTC polarization conversion is analyzed in detail.

2. Design and simulation

The proposed polarization conversion metasurface consists of one layer of patterned metal film printed on a grounded dielectric substrate and covered with a dielectric layer, which is a two-dimensional (2D) square lattice periodic structure, one of its unit cells is illustrated in Fig. 1. It is indicated that the proposed polarization conversion metasurface is an orthotropic structure with a pair of mutually perpendicular symmetric axes *u* and *v* along the directions with the tilt angles of ±45 with respect to the vertical *y* axis. In addition, the geometrical parameters of the unit cell structure are shown in Fig. 1(b). In our design, these geometrical parameters are chosen as follows: $P = 8.00$ mm, $w_1 = 4.2$ mm, $w_2 = 2.5$ mm, $h_1 = 3.0$ mm, and $h_2 = 4.2$ mm; in addition, the two dielectric layers have both a dielectric constant $\varepsilon_r = 2.0$ and a loss tangent $\tan \delta = 0.0018$; moreover, the thickness values of the metallic patterns are all $t = 0.017$ mm.
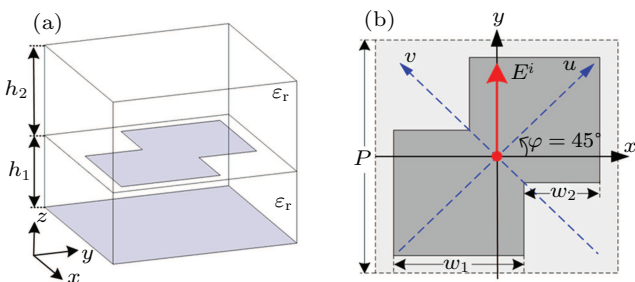

Fig. 1. Unit cell of proposed polarization conversion metasurface: (a) three-dimensional (3D) view, and (b) top view.

To numerically investigate the LTC polarization conversion performance of our design, a series of numerical simulations is carried out by using Ansoft HFSS. Firstly, it is simulated under the *y*-polarized normal incidence. For the *y*-polarized incidence, the co- and cross-polarization reflection coefficient are defined as $r_{yy} = E_y^r/E_y^i$ and $r_{xy} = E_x^r/E_y^i$, respectively. The obtained simulated results, the phase difference $\Delta\varphi_{yx} = \arg(r_{yy}) - \arg(r_{xy})$, together with the magnitudes of r_{xy} and r_{yy}, are shown in Fig. 2. In Fig. 2(a), it is indicated that the phase difference $\Delta\varphi_{yx}$ between r_{xy} and r_{yy} is almost always equal to $+90°$ in the band 5.0 GHz–21.5 GHz; furthermore, figure 2(b) shows that the magnitudes of r_{xy} and r_{yy} are basically equal to each other in the frequency range from 6.0 GHz to 21.0 GHz, it is implied that the reflected wave is close to a left-hand circular-polarized (LHCP) wave in the ultra-wideband frequency band 6.0 GHz–21.0 GHz, for it travels in the $+z$ direction.
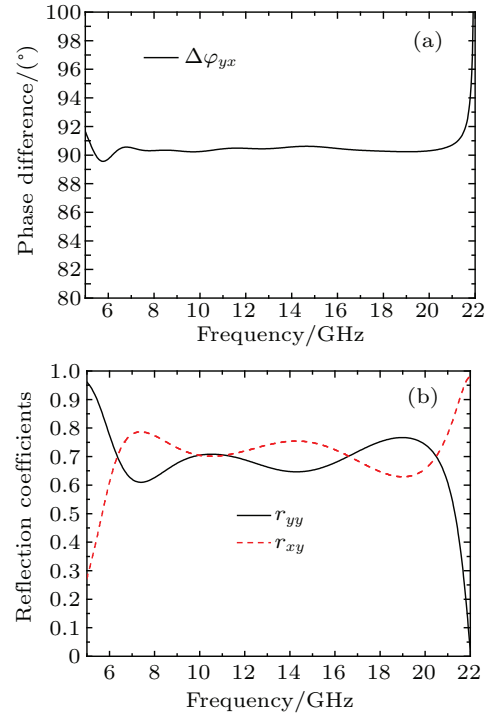

Fig. 2. Simulated results of proposed polarization conversion metasurface under *y*-polarized normal incidence: (a) phase difference $\Delta\varphi_{yx}$ between r_{xy} and r_{yy} and (b) magnitude of r_{xy} and r_{yy}.

In fact, the reflected wave is still not a perfect CP one, but it can be considered as a CP one when its AR is lower than 3.0 dB. According to the relevant literature,[38] the AR of the reflected wave can be calculated from the following equation:

$$\mathrm{AR} = \left(\frac{|r_{yy}|^2 + |r_{xy}|^2 + \sqrt{a}}{|r_{yy}|^2 + |r_{xy}|^2 - \sqrt{a}} \right)^{1/2}, \tag{1}$$

where

$$a = |r_{yy}|^4 + |r_{xy}|^4 + 2|r_{yy}|^2 |r_{xy}|^2 \cos(2\Delta\varphi_{yx}).$$

Based on the simulated results in Fig. 2, the AR of the reflected wave can be calculated out, which is shown in Fig. 3, it is indicated that the AR is lower than 3.0 dB in the frequency range from 5.87 GHz to 21.13 GHz, and the anticipated LTC polarization conversion is realized in the ultra-wideband frequency band, which is corresponding to a 113% relative bandwidth.
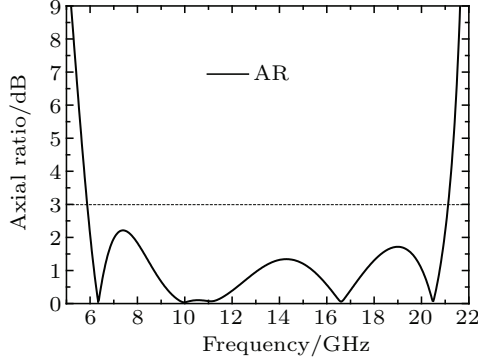

Fig. 3. Axial ratio of reflected wave under y-polarized normal incidence.

Though the reflected wave can be regarded as an LHCP wave when its AR is less than 3.0 dB, it still contains both RHCP component and LHCP component. By using the co- and cross-polarization reflection coefficients under the y-polarized incidence $E^{i} = E_{y}^{i}\hat{e}_{y}e^{-jkz}$, the reflected wave can be expressed as

$$
\begin{aligned}
\boldsymbol{E}_r|_{\boldsymbol{E}_i=E_y^i\hat{e}_y} &= E_y^i(r_{xy}\hat{e}_x + r_{yy}\hat{e}_y) \\
&= \frac{E_y^i\sqrt{2}(r_{xy}+ir_{yy})}{2}\frac{\sqrt{2}(\hat{e}_x - i\hat{e}_y)}{2} \\
&\quad + \frac{E_y^i\sqrt{2}(r_{xy}-ir_{yy})}{2}\frac{\sqrt{2}(\hat{e}_x + i\hat{e}_y)}{2}. \quad (2)
\end{aligned}
$$

Now, if two LTC polarization conversion reflection coefficients are defined as $r_{\mathrm{RHCP}-y} = E_{\mathrm{RHCP}}^r/E_y^i$ and $r_{\mathrm{LHCP}-y} = E_{\mathrm{LHCP}}^r/E_y^i$ respectively, equation (2) shows that the two reflection coefficients can be obtained from the following equation:

$$
\begin{aligned}
r_{\mathrm{RHCP}-y} &= \sqrt{2}\,(r_{xy}+ir_{yy})/2, \\
r_{\mathrm{LHCP}-y} &= \sqrt{2}\,(r_{xy}-ir_{yy})/2. \quad (3)
\end{aligned}
$$

According to the above simulated results, the two LTC polarization conversion reflection coefficients of the proposed polarization conversion metasurface are obtained from Eq. (3), and the magnitudes of the two reflection coefficients are shown in Fig. 4(a), it is implied that the magnitude of the LHCP component is much larger than that of the RHCP component in the

reflected wave. In addition, in order to show the LTC polarization conversion performance of the polarization conversion metasurface in detail, the polarization conversion rate (PCR) is calculated from the following equation:

$$
\mathrm{PCR} = \frac{|r_{\mathrm{LHCP}-y}|^2}{|r_{\mathrm{RHCP}-y}|^2 + |r_{\mathrm{LHCP}-y}|^2}. \quad (4)
$$

The calculated results, shown in Fig. 4(b), indicates that the PCR is kept larger than 97.14% in the whole 3-dB-AR-band. Why is that so? In fact, by using the two LTC polarization conversion reflection coefficients: $r_{\mathrm{RHCP}-y}$ and $r_{\mathrm{LHCP}-y}$, the AR of the reflected wave can be expressed as

$$
\mathrm{AR} = \frac{|r_{\mathrm{LHCP}-y}| + |r_{\mathrm{RHCP}-y}|}{||r_{\mathrm{LHCP}-y}| - |r_{\mathrm{RHCP}-y}||}. \quad (5)
$$

In this way, through the following derivation, it can be well known that the PCR will be kept larger than 97.14% and the magnitude of $r_{\mathrm{RHCP}-y}$ or $r_{\mathrm{LHCP}-y}$ will be less than -15.43 dB in the 3-dB-AR-band of any LTC polarization converter.
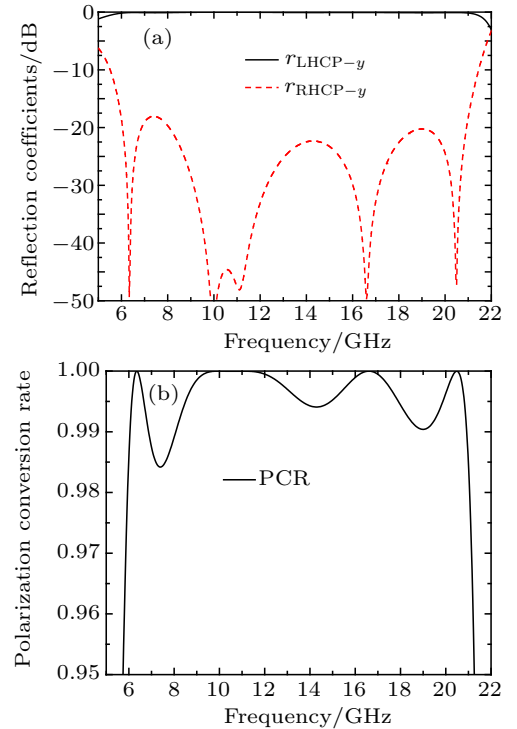

Fig. 4. (a) LTC reflection coefficients and (b) polarization conversion rate (PCR) of proposed polarization conversion metasurface under y-polarized normal incidence.

$$
\mathrm{AR} = \frac{|r_{\mathrm{LHCP}-y}| + |r_{\mathrm{RHCP}-y}|}{||r_{\mathrm{LHCP}-y}| - |r_{\mathrm{RHCP}-y}||} \leq \sqrt{2} \Rightarrow \frac{|r_{\mathrm{LHCP}-y}|}{|r_{\mathrm{RHCP}-y}|} \quad \text{or} \quad \frac{|r_{\mathrm{CHCP}-y}|}{|r_{\mathrm{LHCP}-y}|} \leq 0.1716, \quad (6)
$$

$$
\mathrm{PCR} = \frac{|r_{\mathrm{LHCP}-y}|^2}{|r_{\mathrm{RHCP}-y}|^2 + |r_{\mathrm{LHCP}-y}|^2} \geq \frac{1}{1^2 + 0.1716^2} \geq 97.14\%, \quad (7)
$$

$$
|r_{\mathrm{RHCP}-y}|^2 \quad \text{or} \quad |r_{\mathrm{LHCP}-y}|^2 \leq \sqrt{100\% - 97.14\%} \Rightarrow |r_{\mathrm{RHCP}-y}| \quad \text{or} \quad |r_{\mathrm{LHCP}-y}| \leq -15.43 \ \mathrm{dB}. \quad (8)
$$

However, for the proposed polarization conversion metasurface, figures 4(a) and 4(b) show that the PCR is larger than 99% and the magnitude of $r_{\mathrm{RHCP}-y}$ is less than -20 dB in the wide frequency range from 8.08 GHz to 20.92 GHz, which shows that the proposed polarization conversion metasurface has not only wider bandwidth but also higher efficiency.

3. Theoretical analysis

Why can the proposed polarization conversion metasurface perform such an ultra-wideband and high-efficiency LTC polarization conversion? To obtain a physical insight into the root cause, we carry out a detailed theoretical analysis in the following. As the proposed polarization conversion metasurface is an orthotropic anisotropic structure with a pair of mutually perpendicular symmetric axes u and v, no cross-polarized reflection components will exist under u- and v-polarized incidences, the magnitudes of r_{uu} and r_{vv} will both be very close to 1.0 because of the little dielectric loss. Therefore, in the case of neglecting the little dielectric loss, the following equation can be established:

$$r_{vv} = r_{uu}\mathrm{e}^{-\mathrm{j}\Delta\varphi_{uv}}, \tag{9}$$

where $\Delta\varphi_{uv}$ represents the phase difference between r_{uu} and r_{vv}, which can be limited between r_{uu} and r_{vv}. In addition, as the symmetric axes u and v are along the directions with the tilt angles of $\pm 45°$ with respect to the y axis, the y- and x-polarized unit waves can be expressed as $\hat{e}_y = (\sqrt{2}/2)(\hat{e}_u + \hat{e}_v)$ and $\hat{e}_x = (\sqrt{2}/2)(\hat{e}_u - \hat{e}_v)$, respectively. In this way, when the incident wave is supposed to be a y-polarized one $E^i = E_0\hat{e}_y = E_0(\sqrt{2}/2)(\hat{e}_u + \hat{e}_v)$, the total reflected wave can be expressed as

$$
\begin{aligned}
\boldsymbol{E}^{\mathrm{r}} &= E_u^{\mathrm{r}}\hat{e}_u + E_v^{\mathrm{r}}\hat{e}_v \\
&= \frac{\sqrt{2}}{2}E_0\left(r_{uu}\hat{e}_u + r_{vv}\hat{e}_v\right) \\
&= \frac{\sqrt{2}}{4}E_0\left[(r_{uu}+r_{vv})(\hat{e}_u+\hat{e}_v) + (r_{uu}-r_{vv})(\hat{e}_u-\hat{e}_v)\right] \\
&= E_0\frac{1}{2}(r_{uu}+r_{vv})\hat{e}_y + E_0\frac{1}{2}(r_{uu}-r_{vv})\hat{e}_x,
\end{aligned} \tag{10}
$$

which implies that the co- and cross-polarization reflection coefficient under the y-polarized incidence can be expressed, respectively, as

$$
\begin{aligned}
r_{yy} &= \frac{1}{2}(r_{uu}+r_{vv}) = \frac{1}{2}r_{uu}(1+\mathrm{e}^{-\mathrm{j}\Delta\varphi_{uv}}), \\
r_{xy} &= \frac{1}{2}(r_{uu}-r_{vv}) = \frac{1}{2}r_{uu}(1-\mathrm{e}^{-\mathrm{j}\Delta\varphi_{uv}}).
\end{aligned} \tag{11}
$$

After a similar derivation under x-polarized incidence, the total reflection matrix $\boldsymbol{R}_{\mathrm{lin}}$ in the X–Y coordinate system is obtained as follows:

$$\boldsymbol{R}_{\mathrm{lin}} = \begin{pmatrix} r_{xx} & r_{xy} \\ r_{yx} & r_{yy} \end{pmatrix} = \frac{1}{2}\begin{pmatrix} r_{uu}+r_{vv} & r_{uu}-r_{vv} \\ r_{uu}-r_{vv} & r_{uu}+r_{vv} \end{pmatrix}$$

$$= \frac{1}{2}r_{uu}\begin{pmatrix} 1+\mathrm{e}^{-\mathrm{j}\Delta\varphi_{uv}} & 1-\mathrm{e}^{-\mathrm{j}\Delta\varphi_{uv}} \\ 1-\mathrm{e}^{-\mathrm{j}\Delta\varphi_{uv}} & 1+\mathrm{e}^{-\mathrm{j}\Delta\varphi_{uv}} \end{pmatrix}. \tag{12}$$

According to Eq. (12), the following equation can be established

$$\frac{r_{yy}}{r_{xy}} = \frac{r_{xx}}{r_{yx}} = \frac{1+\mathrm{e}^{-\mathrm{j}\Delta\varphi_{uv}}}{1-\mathrm{e}^{-\mathrm{j}\Delta\varphi_{uv}}} = \frac{\mathrm{e}^{\mathrm{j}\Delta\varphi_{uv}/2}+\mathrm{e}^{-\mathrm{j}\Delta\varphi_{uv}/2}}{\mathrm{e}^{\mathrm{j}\Delta\varphi_{uv}/2}-\mathrm{e}^{-\mathrm{j}\Delta\varphi_{uv}/2}}. \tag{13}$$

Due to $-180° < \Delta\varphi_{uv} < +180°$, $\Delta\varphi_{uv}/2$ will be between $-90°$ and $+90°$. When $0° < \Delta\varphi_{uv}/2 < 90°$, it is indicated in Fig. 5(a) that the phase difference between the co- and cross-polarization reflection coefficient under x- and y-polarized incidences will be $-90°$; however, when $-90° < \Delta\varphi_{uv}/2 < 0°$, figure 5(b) indicates that the phase difference will be $+90°$. From the above analyses, one can well know why the phase difference between r_{xy} and (r_{yy}) is always equal to in the band 5.0 GHz–21.5 GHz. Furthermore, the relation $r_{yy}/r_{xy} = r_{xx}/r_{yx}$ appears in Eq. (13), and it is shown that the ratio of y- to x-polarized reflected component under the y-polarized incidence is always equal to that of x- to y-polarized reflected component under the x-polarized incidence, which implies that when an anisotropic metasurface can convert a y-polarized incident wave into an RHCP/LHCP reflected one, the LTC polarization conversion under x-polarized incidence can be realized at the same time, however, the x-polarized incident wave will be converted into an LHCP/RHCP reflected one.
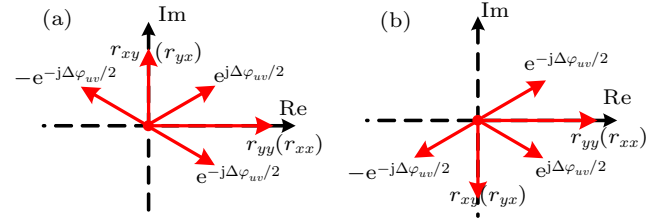

Fig. 5. Intuitive schematic diagram of phase difference between co- and cross-polarization reflection coefficients under x- and y-polarized incidences.

In addition, based on Eq. (12), the magnitudes of r_{yy}, r_{xx} and r_{xy}, r_{yx} can be expressed as

$$
\begin{aligned}
|r_{yy}| &= |r_{xx}| = \frac{1}{2}|r_{uu}|\left|1+\mathrm{e}^{-\mathrm{j}\Delta\varphi_{uv}}\right| \\
&= \frac{1}{2}|1+\cos(\Delta\varphi_{uv})-\mathrm{j}\sin(\Delta\varphi_{uv})| \\
&= \sqrt{(1+\cos\Delta\varphi_{uv})/2}, \\
|r_{xy}| &= |r_{yx}| = \frac{1}{2}|r_{uu}|\left|1-\mathrm{e}^{-\mathrm{j}\Delta\varphi_{uv}}\right| \\
&= \frac{1}{2}|1-\cos(\Delta\varphi_{uv})+\mathrm{j}\sin(\Delta\varphi_{uv})| \\
&= \sqrt{(1-\cos\Delta\varphi_{uv})/2}.
\end{aligned} \tag{14}
$$

Because $+90°$ phase difference will always exist between the co- and cross-polarization reflection coefficients under x- and y-polarized incidences, now equation (14) implies that the magnitude of the co- and cross-polarization reflection coefficients will be equal to each other when $\Delta\varphi_{uv} = \pm 90°$, so that a perfect LTC polarization conversion will be realized in the

reflected wave at this time. However, the magnitude of the co- and cross-polarization reflection coefficients will not be equal to each other in common cases, thus the reflected wave will be an elliptically polarized one, whose AR can be expressed as

$$AR = \sqrt{(1 \pm \cos\Delta\varphi_{uv})/(1 \pm \cos\Delta\varphi_{uv})}, \tag{15}$$

where the choice of addition or subtraction symbol depends on wheteher the AR is ensured to be never less than 1.0. In addition, when $\Delta\varphi_{uv} = \pm180°$, the magnitude of r_{yy} and r_{xx} will be equal to zero, so that a cross polarization conversion will be realized. Why can a perfect LTC polarization conversion be realized when $\Delta\varphi_{uv} = \pm90°$? In fact, under x- and y-polarized incidences, in the case of neglecting the little dielectric loss, the incident wave and reflected wave both can be regarded as a composite wave composed of u- and v-polarized components with equal amplitude, the two orthogonal components in the incident wave are in phase with each other, however, in the reflected wave, the phase difference between the two orthogonal components will be changed: when $\Delta\varphi_{uv} = \pm90°$, the phase difference will be changed to $\pm90°$, so the perfect LTC polarization conversion will be realized.
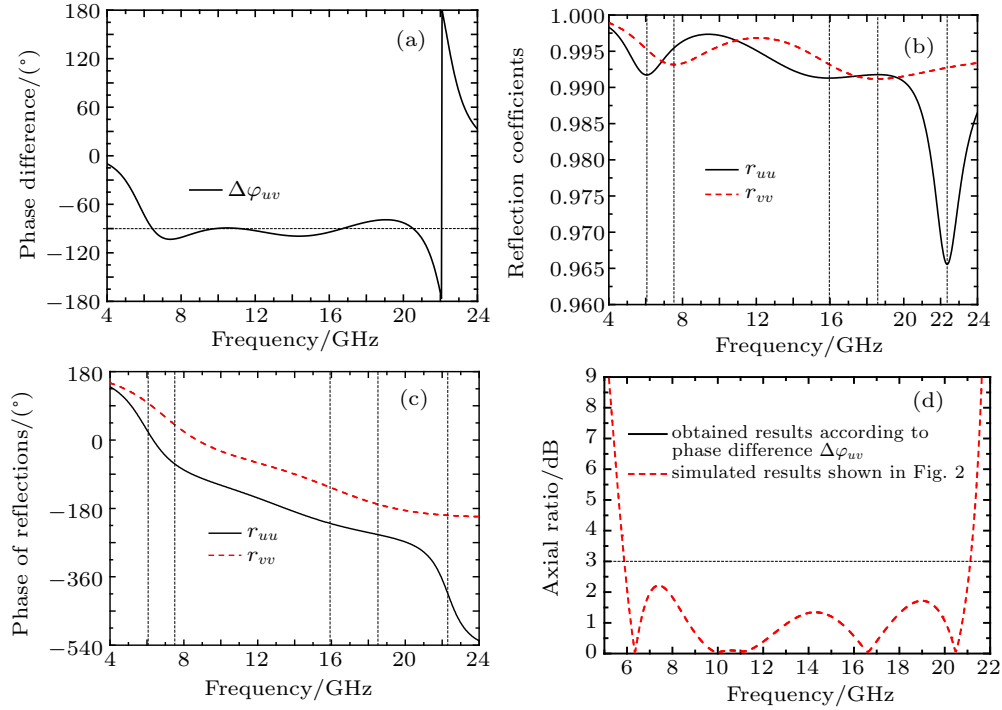

Fig. 6. Simulated results of proposed polarization conversion metasurface under u- and v-polarized normal incidences: (a) phase difference between r_{uu} and r_{vv}, (b) magnitudes and (c) phases of r_{uu} and r_{vv}, (d) axial ratio (AR) of the reflected wave.

According to the above analysis, to make clear the root cause of the LTC polarization conversion for the proposed polarization conversion metasurface, the related simulation is carried out under u- and v-polarized incidences. The simulated results, $i.e.$, the phase difference $\Delta\varphi_{uv}$ between r_{uu} and r_{vv}, is shown in Fig. 6(a). It is indicated that the phase difference $\Delta\varphi_{uv}$ always stays close to $-90°$ in a frequency range between 6.0 GHz and 21.0 GHz, which implies that the anticipanted LTC polarization conversion will be realized in the ultra-wide frequency band. Why is the obtained $\Delta\varphi_{uv}$ so good? To see the cause, the other simulated results, $i.e.$, the magnitudes of r_{uu} and r_{vv}, together with their phases, are shown in Figs. 6(b) and 6(c). Figure 6(b) shows that the magnitude of r_{uu} and r_{vv} are both close to 1.0 at all frequencies, which verifies that the dielectric loss of the proposed polarization conversion metasurface is little; however, the curves of r_{uu} and r_{vv} each still have a certain quantity of fluctuation and have three and two local minimum values respectively, which are located at 6.07, 15.95, 22.35, 7.56, and 18.55 GHz, respectively, it is

implied that there are three and two resonant modes excited by u- and v-polarized incidences, respectively, thereby causing these local maximum dielectric losses. In addition, the curvatures of the curves of r_{uu} and r_{vv} at different resonant frequencies are quite different, which implies that these resonant modes have different Q values. Furthermore, in Fig. 6(c), it is shown that the phase change rate of r_{uu} or r_{vv} at each resonant frequency is different, it is just because of the difference in Q value among these resonant modes. According to the phase change rate shown in Fig. 6(c), the phase difference $\Delta\varphi_{uv}$ can stay close to $-90°$ in a frequency range between 6.0 GHz and 21.0 GHz, which is mainly because of the following two reasons: Firstly, compared with the first resonant mode (7.56 GHz) under v-polarized incidence, the first resonant mode (6.07 GHz) under u-polarized incidence has not only lower resonant frequency but also higher Q value, which makes the phase of r_{uu} decrease earlier and more rapidly, so the phase difference $\Delta\varphi_{uv}$ can be kept close to $-90°$ in the band of 6.0 GHz–11.0 GHz. Secondly, the Q values of the

two second resonant modes (15.95 GHz, 18.55 GHz) under u- and v-polarized incidences are both very small, moreover, they are basically the same, which results in the same change trends of the phase of r_{uu} and r_{vv} with frequency increasing in the band of 11.0 GHz–21.0 GHz, thus the phase difference $\Delta\varphi_{uv}$ can still be kept close to $-90°$ in the wide subsequent band. Finally, according to the obtained phase difference $\Delta\varphi_{uv}$ in Fig. 6(a), the AR of the reflected wave is calculated from Eq. (15), the obtained results are shown in Fig. 6(d), and it is shown that the obtained AR is essentially in agreement with the one in Fig. 3.

Through the above analysis, it is well understood why the polarization conversion metasurface can perform such a high-efficiency and ultra-wideband LTC polarization conversion, which, apart from the two first resonant modes under u- and v-polarized incidences, can be attributed mainly to the two second resonant modes. The appropriate difference between the two first resonant modes causes the phase difference $\Delta\varphi_{uv}$ to be close to $-90°$ in the band of 6.0 GHz–11.0 GHz, but the similarity, together with the small Q values, of the two second resonant modes leads to $\Delta\varphi_{uv}$ to stay close to $-90°$ in the wide subsequent band of 11.0 GHz–21.0 GHz. In this way, the anticipated LTC polarization conversion is realized in the ultra-wide frequency band of 6.0 GHz–21.0 GHz.

4. Experimental validation

Finally, we fabricated an experimental sample and carried out an experimental validation for our design. The fabri-cated sample is shown in Fig. 7(a), where the inset is a zoom view of one unit cell. Firstly, its co- and cross-polarization reflection coefficients under y-polarized normal incidence have been measured, which was measured in a microwave anechoic chamber by using an Agilent E8363B network analyzer together with a pair of identical standard-gain horn antennas. The schematic illustration of the measurement setup is shown in Fig. 7(b), in which the pair of horn antennas was used to transmit and receive a y-polarized incident wave and its reflected wave, respectively, the sample was irradiated; to carry out the measurement under normal incidence, the separation angle between the orientations of the pair of antennas should ideally be close to $0°$, it was set to be $6°$ for the finite sizes of the fabricated sample. The co- and cross-polarization reflection coefficients under y-polarized normal incidence were measured (R_{yy} and R_{xy}) when the receiving horn antenna was rotated $0°$ and $90°$, respectively. Then, based on the measured R_{yy} and R_{xy}, the AR of the reflected wave was obtained from Eq. (1). Finally, when the transmitting antenna was set to be x-polarized, the AR of the reflected wave under x-polarized incidence was measured through the same experimental steps. In this experiment, the measured results are shown in Fig. 7(c), showing that the measured results under y-polarized incidences are in good agreement with the simulated ones in Fig. 3. In addition, under x- and y-polarized incidences, these measured results are basically the same, which agree well with the theoretical predications.
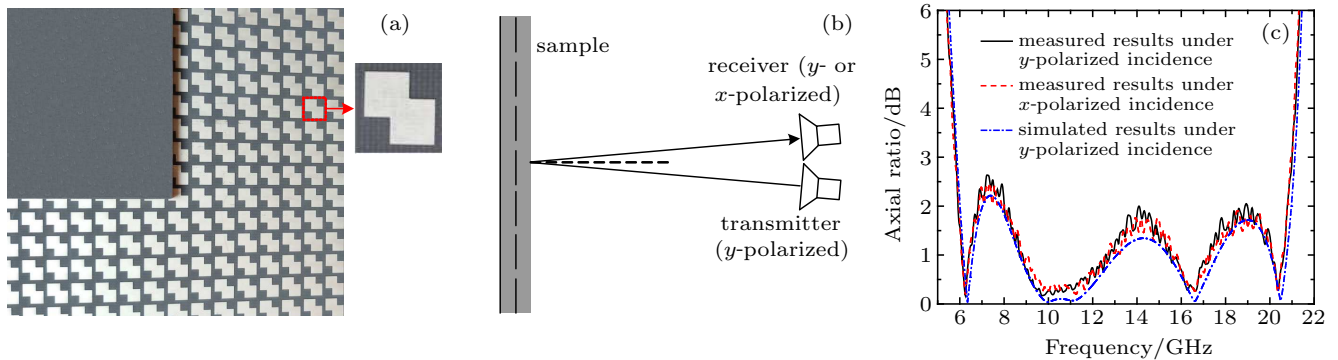

Fig. 7. (a) Photographs of experimental sample, (b) schematic diagram of measurement setup, and (c) measured results: axial ratio (AR) of reflected wave under x- and y-polarized incidences.

5. Conclusions

In this paper, an LTC polarization conversion metasurface is proposed, which can realize high-efficiency and ultra-wideband LTC polarization conversion in the frequency band from 5.87 GHz to 21.13 GHz with a relative bandwidth of 113% under x- and y-polarized incidences, the effective LTC polarization conversion performance is verified through simulations and experiment. In addition, to obtain an insight into the root cause of the LTC polarization conversion, a detailed theoretical analysis is presented, it is indicated that the proposed metasurface can perform an ultra-wideband and high-efficiency LTC polarization conversion, apart from its two first resonant modes under u- and v-polarized incidences, it can be attributed mainly to the two second resonant modes, these resonant modes cause $\Delta\varphi_{uv}$ to stay close to $-90°$ in an ultra-wide frequency band of 6.0 GHz–21.0 GHz, thus the anticipated LTC polarization conversion is realized in the ultra-wide frequency band. Compared with the previous designs, the proposed LTC polarization conversion metasurface has not only ultra-wide bandwidth but also much high efficiency, so it is of great application values for realizing polarization controlled devices, stealth surfaces, antennas, *etc*.

References

[1] Kajiwara A 1995 *IEEE Trans. Veh. Technol.* **44** 487

[2] Chen H, Wang J, Ma H, *et al*. 2015 *Chin. Phys. B* **24** 014201

[3] Gao X, Han X, Cao W, Li H and Ma H 2015 *IEEE Trans. Anten. Propag.* **63** 3522

[4] Zhou G, Tao X, Shen Z, *et al*. 2016 *Sci. Rep.* **6** 38925

[5] Dong G, Shi H, Xia S, Li W, Zhang A, Zhuo X and Wei X 2016 *Chin. Phys. B* **25** 084202

[6] Sun H, Gu C, Chen X, Li Z, Li L and Martion F 2017 *J. Appl. Phys.* **121** 174902

[7] Xu P, Wang S Y and Geyi W 2017 *J. Appl. Phys.* **121** 144502

[8] Jin X, Rongqiang L and Jin Q 2018 *Opt. Express* **26** 20913

[9] Pu Y, Luo Y, Liu L, He D, Xu H, Jing Y and Liu Z 2018 *Chin. Phys. B* **27** 024202

[10] Khan M I and Tahir F A 2018 *Chin. Phys. B* **27** 014101

[11] Lin B, Guo J, Lv L, *et al*. 2019 *Appl. Phys. A* **125** 76

[12] Xu, Li R, Jiang X, Wang S and Han T 2019 *Acta Phys. Sin.* **68** 117801 (in Chinese)

[13] Wang Q, Kong X and Yan X 2019 *Chin. Phys. B* **28** 074205

[14] Li Y, Zhang Q, Qu S, *et al*. 2015 *Chin. Phys. B* **24** 014202

[15] Yang J, Qu S, Ma H, *et al*. 2017 *Appl. Phys. A* **123** 537

[16] Huang X, Chen J and Yang H 2017 *J. Appl. Phys.* **122** 043102

[17] Wang Q, Plum E, Yang Q, Zhang X and Xu Q 2018 *Light: Science & Applications* **7** 25

[18] Lin B, Guo J, Chu P, *et al*. 2018 *Phys. Rev. Appl.* **9** 024038

[19] Huang C, Feng Y, Zhao J, *et al*. 2012 *Phys. Rev. B* **85** 195131

[20] Liu W, Chen S, Li Z, *et al*. 2015 *Opt. Lett.* **40** 3185

[21] Zhou G, Tao X, Shen Z, *et al*. 2016 *Sci. Rep.* **6** 38925

[22] Chen K, Bai Y, Bu T, *et al*. 2016 *Opt. Eng.* **55** 030801

[23] Wang S Y, Liu W and Geyi W 2018 *Sci. Rep.* **8** 3791

[24] Pfeiffer C, Zhang C, Ray V, Guo L J and Grbic A 2014 *Phys. Rev. Lett.* **113** 023902

[25] Wu X, Meng Y, Wang L, Tian J, Dai S and Wen W 2016 *Appl. Phys. Lett.* **108** 183502

[26] Fernández O, Gómez A, *et al*. 2017 *IEEE Anten. & Wireless Propag. Lett.* **16** 2307

[27] Gao X, Yu X Y, Cao W P, Jiang Y N and Yu X H 2016 *Chin. Phys. B* **25** 128102

[28] Jiang Y, Wang L, Wang J, Akwuruoha C and Cao W 2017 *Opt. Express* **25** 27616

[29] Ran Y, Shi L, Wang J, Wang S, Wang G and Liang J 2019 *Opt. Commun.* **451** 124

[30] Fartookzadeh M 2017 *J. Mod. Opt.* **64** 1854

[31] Mao C, Yang Y, He X, *et al*. 2017 *Appl. Phys. A* **123** 767

[32] Zheng Q, Guo C and Ding J 2018 *IEEE Antennas and Wireless Propagation Lett.* **17** 1459

[33] Mahdi F 2018 *Modern Phys. Lett. B* **32** 1850274

[34] Zeng L, Liu G, Zhang H and Huang T 2019 *Acta Phys. Sin.* **68** 054101 (in Chinese)

[35] Li Y, Zhang J, Qu S, Wang J, *et al*. 2015 *J. Appl. Phys.* **117** 044501

[36] Baena D, Glybovski B, del Risco P, Slobozhanyuk P and Belov A 2017 *IEEE Trans. Anten. Propag.* **65** 4124

[37] Baena J, Risco J D, Slobozhanyuk A and Belov P 2015 *Phys. Rev. B* **92** 245413

[38] Abadi S and Behdad N 2016 *IEEE Trans. Anten. Propag.* **64** 525

[39] Wu J L, Lin B Q and Da X Y 2016 *Chin. Phys. B* **25** 088101

[40] Lin B, Wu J, Da X, *et al*. 2017 *Appl. Phys. A* **123** 43

[41] Jiang W and Wen W 2017 *Opt. Express* **25** 3805

[42] Zhang W, Li J Y and Xie J 2017 *IEEE Trans. Anten. Propag.* **65** 5623

[43] Lin B, Guo J, Huang B, Fang L and Chu P 2018 *Chin. Phys. B* **27** 054204

[44] Akgol O, Unal E, Altintas O, *et al*. 2018 *Optik* **161** 12